

Photon Splitting in Strongly Magnetized Plasma

Tomasz Bulik

Nicolaus Copernicus Astronomical Center, Bartycka 18, 00-716 Warsaw, Poland

ABSTRACT

The process of photon splitting, becomes allowed in the presence of strong magnetic field. We calculate the influence of magnetized plasma on the photon splitting absorption coefficient. We calculate the refraction coefficients and polarization vectors with the inclusion of the vacuum terms at an arbitrary value of the magnetic field, and then find photon splitting matrix element taking into account the terms that vanish in vacuum, but may be nonzero in the presence of plasma. We find the photon splitting rate in plasma with the density typical for a neutron star star atmosphere and identify a region of the parameter space where the plasma effects are important.

1. Introduction

The possibility of photon splitting process in strong magnetic field around $B_c = 4.414 \times 10^{13}$ Gauss has been first noted in the early seventies (Adler 1971, Białynicka-Birula & Białynicki-Birula 1970). Adler (1971) found that only one type of splitting is allowed, namely $\perp \rightarrow \parallel + \parallel$, where a perpendicularly polarized photon splits into two parallel polarized photons. This calculation took into account the vacuum dispersion and also the influence of matter with density that of a pulsar magnetosphere. The normal modes are polarized linearly in such conditions. The photon splitting absorption coefficient for this allowed reaction is

$$\kappa = 0.12 \left(\frac{B}{B_c} \sin \theta \right)^6 \left(\frac{\hbar \omega}{mc^2} \right)^5. \quad (1)$$

Since then a number of authors have derived the matrix elements, and absorption coefficients for this process using different approaches (Papanyan & Ritus 1972, Stoneham 1979) and also recently (Baier, Milshtein & Shaisultanov 1996, Baring & Harding 1997). These papers have settled the controversy sparked by Mentzel, Berg & Wunnner (1994) who suggested that the photon splitting rate may actually be a few orders of magnitude higher than previously thought.

This exotic process has found a number of astrophysical applications. A natural environment where it may play a role is provided by neutron stars, since a number of them have magnetic fields in excess of 10^{12} Gauss, and about a dozen of radio pulsars has spin down fields larger than 10^{13} Gauss. It has been found that photon splitting plays an important role in the formation of the gamma ray spectrum of PSR 1509-58, where it inhibits emission above 1 MeV (Harding, Baring & Gonthier 1997). Soft gamma-ray repeaters (SGR) form another class of objects where

photon splitting has been suggested to play an important role. There were three firmly established SGR's with and the fourth source was recently discovered (Kouveliotou 1997). All of them are characterized by short durations, below a second, and spectra with cut-offs around 30 keV. A number of arguments have been presented (Thompson & Duncan 1995) pointing that these sources are actually *magnetars*, i.e. neutron stars with magnetic fields reaching 10^{15} Gauss, for which the main pool of energy is the magnetic field. Baring (1995) suggested that photon splitting may be responsible for the spectral cutoffs in the spectra of SGRs, invoking a possibility of photon splitting cascades. Thompson and Duncan (1995) showed that even in the absence of cascades photon splitting influences the shape of the spectra of SGRs.

In this work we investigate the process of photon splitting not only in vacuum but also in the presence of matter with the density like that in a neutron star atmosphere, when the plasma dispersion may be important and for some range of propagation directions the normal modes are polarized circularly. The relevance of plasma effects can have a very substantial influence on the absorption coefficients. For example, Bulik and Miller (1997) have shown that plasma effects leads to a broad absorption like feature below ≈ 10 keV for a large range of SGR emission models. In section 2 we analyze the polarization of the normal modes in the strongly magnetized plasma, in section 3 we calculate the photon splitting matrix elements and absorption coefficients, in section 4 we present the results and we discuss them in section 5.

2. Polarization of the normal modes, refraction coefficient

We use the normal mode formalism to describe opacities in strong magnetic field. The dispersion equation is

$$\vec{k} \times [\mu^{-1} (\vec{k} \times \vec{E})] + \left(\frac{\omega}{c}\right)^2 \epsilon \vec{E} = 0, \quad (2)$$

where ϵ is the electric permittivity tensor, μ is the magnetic permeability tensor and \vec{E} is the electric field of the wave. Equation (2) has been discussed by e.g. Ginzburg & Ruchadze 1975, and Meszaros (1992). In general equation (2) has three solutions: one representing the longitudinal plasma oscillations that do not propagate (Meszaros 1992, p.69), and two perpendicular representing the electromagnetic waves. In the presence of the magnetic field there exist two nondegenerate wave solutions of equation (2), and therefore the medium is birefringent. We follow the convenient method introduced by Gnedin & Pavlov (1974) for the case of tenuous plasma to solve equation (2).

The roots of the dispersion equation are

$$n_j = n_I \pm \sqrt{n_L^2 + n_C^2}, \quad (3)$$

where $j = 1, 2$ indicates which normal mode is selected. The refraction coefficients are given by the real part of n_j , and the total absorption coefficients are proportional to the imaginary part of

n_j ; $\xi_j = (2\omega/c)\text{Im}(n_j)$, and

$$\begin{aligned} n_I \equiv & 1 + \frac{1}{4}(\epsilon_{xx} + \epsilon_{yy} \cos^2 \theta + \epsilon_{zz} \sin^2 \theta - \epsilon_{xz} \sin 2\theta \\ & - \mu_{xx}^{-1} - \mu_{yy}^{-1} \cos^2 \theta - \mu_{zz}^{-1} \sin^2 \theta + \mu_{xz}^{-1} \sin 2\theta), \end{aligned} \quad (4)$$

$$\begin{aligned} n_L \equiv & \frac{1}{4}(\epsilon_{xx} - \epsilon_{yy} \cos^2 \theta - \epsilon_{zz} \sin^2 \theta + \epsilon_{xz} \sin 2\theta \\ & + \mu_{xx}^{-1} - \mu_{yy}^{-1} \cos^2 \theta - \mu_{zz}^{-1} \sin^2 \theta + \mu_{xz}^{-1} \sin 2\theta), \end{aligned} \quad (5)$$

$$n_C \equiv \frac{i}{2}(\epsilon_{xy} \cos \theta + \epsilon_{xz} \sin \theta). \quad (6)$$

Here μ_{ab}^{-1} is the ab component of the inverse μ tensor, and we use the system of coordinates with the magnetic field along the z -axis, and the wave vector in the yz plane at an angle θ to the magnetic field.

We describe the polarization of the normal modes by the position angle χ_j between the major axis of the polarization ellipse and the projection of the magnetic field \vec{B} on the plane perpendicular to the wave vector \vec{k} , and the ellipticity \mathcal{P} , whose modulus is equal to the ratio of the minor axis to the major axis of the polarization ellipse, and whose sign determines the direction of rotation of the electric field:

$$\mathcal{P}_j = \frac{r_j - 1}{r_j + 1}, \quad r_j \exp(2i\chi_j) = \frac{-n_C \pm \sqrt{n_L^2 + n_C^2}}{n_L}.$$

The polarization vectors can be described by a complex variable b , or by two real parameters q and p (Pavlov, Shibanov, & Yakovlev 1980)

$$b \equiv q + ip = \frac{n_L}{n_C}. \quad (7)$$

Let us consider a wave travelling in the direction described by θ and ϕ in the coordinate system with the magnetic field along the z -axis, and the x -axis chosen arbitrarily. The wave vector is $\vec{k} = k(\cos \theta, \sin \theta \sin \phi, \sin \theta \cos \phi)$. In the rotating coordinate system $e_{\pm} = 2^{-1/2}(e_x \pm ie_y)$, $e_0 = e_z$, the polarization vectors are

$$\begin{aligned} e_{\pm}^j &= i^{j+1} \frac{1}{\sqrt{2}} C_j e^{\mp i\phi} (K_j \cos \theta \pm 1) \\ e_0^j &= C_j K_j \sin \theta \end{aligned} \quad (8)$$

where

$$K_j = b \left[1 + (-1)^j \left(1 + b^{-2} \right)^{1/2} \right] \quad (9)$$

and $C_j = (1 + |K_j|^2)^{-1/2}$. In general K_j are complex.

2.1. Vacuum polarization effects

We use the convention where we label the polarization state by the direction of the electric field vector of the wave in relation to the external magnetic field. Adler (1971) used a different convention using the magnetic, not electric field of the wave to define polarization.

The refraction indices in strong magnetic field have been derived by Adler (1971). The result is

$$n_{\parallel,\perp}^{vac} = 1 - \frac{1}{2} \sin^2 \theta A^{\parallel,\perp}(\omega \sin \theta, B), \quad (10)$$

where the functions $A^{\parallel,\perp}$ are rather lengthy double integrals given by equation (51) in Adler (1971):

$$A^{\parallel,\perp}(\omega, B) = \frac{\alpha}{2\pi} \int_0^\infty \frac{ds}{s^2} \exp(-s) \int_0^s \exp[\omega^2 R(s, t)] J^{\parallel,\perp}(s, v) \quad (11)$$

and $v = 2ts^{-1} - 1$. The remaining functions $J^{\parallel,\perp}$ are

$$J^\perp(s, v) = -\frac{Bs \cosh(Bsv)}{\sinh(Bs)} + \frac{Bsv \sinh(Bsv) \coth(Bs)}{\sinh(Bs)} + -\frac{2Bs[\cosh(Bsv) - \cosh Bs]}{\sinh^3(Bs)} \quad (12)$$

$$J^\parallel = \frac{Bs \cosh(Bsv)}{\sinh(Bs)} - Bs \coth(Bs) \left[1 - v^2 + v \frac{\sinh(Bsv)}{\sinh(Bs)} \right]. \quad (13)$$

The function R is given by

$$R(s, t) = \frac{1}{2} \left[2t \left(1 - \frac{t}{s} \right) + \frac{\cosh(Bsv) - \cosh(Bs)}{B \sinh(Bs)} \right]. \quad (14)$$

The refraction indices $n_{1,2}^{vac} = 1 + \eta \sin^2 \theta$ have been calculated for $\hbar\omega \ll m_e c^2$ and arbitrary magnetic field by Tsai & Erber (1974) In the low field limit, $B \ll B_c$,

$$\begin{aligned} \eta_\parallel(h) &\approx \frac{14}{45} h^2 - \frac{13}{315} h^4 \\ \eta_\perp(h) &\approx \frac{8}{45} h^2 - \frac{379}{5040} h^4, \end{aligned}$$

and when $B \gg B_c$

$$\begin{aligned} \eta_\parallel(h) &\approx \frac{2}{3} h + \left(\frac{1}{3} + \frac{2}{3} \gamma - 8L_1 \right) \\ \eta_\perp(h) &\approx \frac{2}{3} - h^{-1} \ln(2h), \end{aligned}$$

where $h = B/B_c$, and $L_1 = 0.249..$, and $\gamma = 0.577..$ is the Euler's constant (Tsai & Erber 1974). Thus in the limit of strong magnetic field refraction for the parallel mode grows linearly with the field while that of the perpendicular mode is nearly constant. We present the dependence of the vacuum refraction coefficients as a function of the magnetic field in Figure 1.

We have evaluated numerically the integrals of equations (10). Figure 2 shows the dependence of the refraction coefficients on the photon energy for a few magnetic fields.

2.2. Refraction coefficient in the system of plasma and vacuum

Plasma in strong magnetic field can be described by the dielectric tensor

$$\epsilon_{ab} = \epsilon_{ab}^{vac} + \epsilon_{ab}^p - \delta_{ab},$$

and the vacuum permeability tensor. The plasma dielectric tensor can be expressed as

$\epsilon_{ab} = \delta_{ab} - \left(\frac{\omega_p^2}{\omega^2} \right) \Pi_{ab}$, where $\omega_p = \left(\frac{4\pi Ne^2}{m} \right)^{1/2}$ is the plasma frequency and Π_{ab} is the plasma polarization tensor. The plasma polarization tensor is diagonal in the rotating coordinates, and for cold electron plasma is given by

$$\Pi_{\alpha\alpha} = \frac{\omega}{\omega + \alpha\omega_B - i\gamma_r} = \frac{\omega}{\omega_t + \alpha\omega_B}, \quad (15)$$

where $\alpha = -1, 0, +1$, and $\gamma_r = (2/3)(e^2/mc^3)\omega^2$ is the radiative width, and we denote $\omega_t = \omega - i\gamma_r$. Inserting equation (15) into equations (5) and (6), we obtain

$$n_I = 1 - \frac{1}{4} \frac{\omega_p^2}{\omega} \left[(1 + \cos^2 \theta) \frac{\omega_t}{\omega_t^2 - \omega_B^2} + \sin^2 \theta \frac{1}{\omega_t} \right] + \frac{1}{4} (A^{\parallel}(\omega \sin \theta, B) + A^{\perp}(\omega \sin \theta, B)), \quad (16)$$

$$n_L = -\frac{\sin^2 \theta}{4} \times \left\{ \frac{\omega_p^2}{\omega \omega_t} \frac{\omega_B^2}{\omega_t^2 - \omega_B^2} + [A^{\parallel}(\omega \sin \theta, B) - A^{\perp}(\omega \sin \theta, B)] \right\} \quad (17)$$

and

$$n_C = -\frac{1}{2} \frac{\omega_p^2}{\omega} \left(\frac{\omega_B}{\omega_t^2 - \omega_B^2} \right) \cos \theta. \quad (18)$$

Inserting equations (17) and (18) into equation (7), and neglecting terms proportional to γ_r^2 we obtain

$$q = \frac{\sin^2 \theta}{2 \cos \theta} \frac{\omega_B}{\omega} \left[1 - (A^{\parallel}(\omega \sin \theta, B) - A^{\perp}(\omega \sin \theta, B)) \frac{\omega^2}{\omega_p^2} \left(\frac{\omega^2}{\omega_B^2} - 1 \right) \right] \quad (19)$$

and

$$p = \frac{\sin^2 \theta}{2 \cos \theta} \times \frac{\omega_B \gamma_r}{\omega^2} \left[1 + 2(A^{\parallel}(\omega \sin \theta, B) - A^{\perp}(\omega \sin \theta, B)) \frac{\omega^2}{\omega_p^2} \right]. \quad (20)$$

polarization vectors and refraction coefficients are determined by equations (16), (17), and (18) combined with (3) and (8).

The presence of matter influences refraction also because of the electron cyclotron resonance at ω_b . These effects increase for propagation direction along the magnetic field, and are proportional to the matter density. For a detailed discussion see e.g. Mészáros (1992).

3. Photon splitting rate

We will use two coordinate systems U , and U' . The z -axis in the system U lies along the magnetic field, and the wave vector of the initial photon is in the zx -plane. The z -axis in the system U' lies along \vec{k} , the wave vector of the initial photon, and the magnetic field lies in the xz -plane. The system U is convenient for calculation of the matrix element M and the refraction indices n_j , while U' will be used for integration. In U the wave vector of the initial photon is $\vec{k}_0 = k_0(\cos \theta_0, 0, \sin \theta_0)$. The vector \vec{k}_1 in U' is $\vec{k}_1 = (\cos \theta', \sin \theta' \sin \phi', \sin \theta' \cos \phi')$, and in U it is $\vec{k}_1 = k_1(\cos \theta_0 \cos \theta' - \sin \theta_0 \sin \theta' \cos \phi', \sin \theta' \sin \phi', \sin \theta_0 \cos \theta' + \cos \theta_0 \sin \theta' \cos \phi')$. Using the momentum conservation we obtain in U' $\vec{k}_2 = \vec{k} - \vec{k}_1$. Polarization vector of a photon is given by $\vec{e}(\vec{k}) = \vec{e}(\omega, \theta, \varphi)$. We calculate the polarization vectors for each photon separately, given its frequency and the direction of propagation.

The photon splitting absorption coefficient can be found by integrating the S -matrix element over the phase space of the final states,

$$r = \int \frac{1}{2} \frac{1}{2\omega} \frac{d^3 k_1}{(2\pi)^3 2\omega_1} \frac{d^3 k_2}{(2\pi)^3 2\omega_2} \frac{|S|^2}{VT}. \quad (21)$$

This can be expressed as

$$r = \frac{2\alpha^6}{(2\pi)^3} \int |\mathcal{M}|^2 \omega \omega_1 \omega_2 d^3 k_1 d^3 k_2 \delta(\sum \omega_i) \delta(\sum \mathbf{k}_i).$$

where the matrix element \mathcal{M} is a function of energies and polarization vectors of the incoming and outgoing photons.

3.1. Matrix elements

We use the system of units in which $\hbar = c = m_e = 1$, so the fine structure constant is $\alpha = e^2$. The magnetic field is expressed in the units of the critical field B_c . The effective Lagrangian of the electromagnetic field with QED corrections is given by (Berestetskii, Lifshits and Pitaevskii 1982)

$$L_{\text{eff}} = \frac{1}{8\pi^2} \int_0^\infty \frac{e^{-\lambda}}{\lambda^3} d\lambda \times \left\{ -(\xi \cot \xi)(\eta \coth \eta) + 1 - \frac{\xi^2 - \eta^2}{3} \right\}. \quad (22)$$

Here

$$\begin{aligned} \xi &= -\lambda \frac{ie}{\sqrt{2}} \left\{ (\mathcal{F} + i\mathcal{J})^{1/2} - (\mathcal{F} - i\mathcal{J})^{1/2} \right\}, \\ \eta &= \lambda \frac{e}{\sqrt{2}} \left\{ (\mathcal{F} + i\mathcal{J})^{1/2} + (\mathcal{F} - i\mathcal{J})^{1/2} \right\}, \end{aligned}$$

and $\mathcal{F} = \frac{1}{2} (\mathbf{B}^2 - \mathbf{E}^2)$, $\mathcal{J} = \mathbf{B} \cdot \mathbf{E}$ are the field invariants. In the low frequency approximation the S -matrix element can be calculated as

$$S_{\gamma \rightarrow \gamma_1 + \gamma_2} = \langle \gamma | \int d\mathbf{r} dt V_{\text{int}} | \gamma_1 \gamma_2 \rangle,$$

where the interaction operator is $V_{\text{int}} = L_{\text{eff}}$.

We find that the two lowest order terms of the S-matrix correspond to a square and hexagon diagrams:

$$S_6 = -i \frac{2\alpha^3 B^3}{(2\pi)^2 315} (4\pi)^{3/2} \times (2\pi)^4 \omega \omega_1 \omega_2 \delta(\sum \omega_i) \delta(\sum \mathbf{k}_i) M_6. \quad (23)$$

and

$$S_4 = i \frac{2\alpha^2}{45(4\pi)^2} (4\pi)^{3/2} B \omega \omega_1 \omega_2 \delta(\sum \omega_i) \delta(\sum \mathbf{k}_i) M_4. \quad (24)$$

The matrix elements are

$$\begin{aligned} M_6 &= 48\mathcal{A} + 26\mathcal{B} + 13\mathcal{C} + 16\mathcal{D}, \\ M_4 &= 8\mathcal{C} + 14\mathcal{D}, \end{aligned}$$

and denoting the by n_i , \mathbf{n}_i , \mathbf{e}_i , the index of refraction, the direction of propagation, and the polarization vector of the i -th photon respectively we obtain:

$$\begin{aligned} \mathcal{A} &= n_0 n_1 n_2 (\mathbf{n}_0 \times \mathbf{e}_0)_z (\mathbf{n}_1 \times \mathbf{e}_1^*)_z (\mathbf{n}_2 \times \mathbf{e}_2^*)_z \\ \mathcal{B} &= n_0 (\mathbf{n}_0 \times \mathbf{e}_0)_z e_{1z}^* e_{2z}^* + n_1 (\mathbf{n}_1 \times \mathbf{e}_1^*)_z e_{0z} e_{2z}^* + n_2 (\mathbf{n}_2 \times \mathbf{e}_2^*)_z e_{0z} e_{1z}^* \\ \mathcal{C} &= n_0 (\mathbf{n}_0 \times \mathbf{e}_0)_z \{ [n_1 n_2 (\mathbf{n}_1 \mathbf{n}_2) - 1] (\mathbf{e}_1^* \mathbf{e}_2^*) - n_1 n_2 (\mathbf{n}_1 \mathbf{e}_2^*) (\mathbf{n}_2 \mathbf{e}_1^*) \} + \\ &\quad n_1 (\mathbf{n}_1 \times \mathbf{e}_1^*)_z \{ [n_0 n_2 (\mathbf{n}_0 \mathbf{n}_2) - 1] (\mathbf{e}_0 \mathbf{e}_2^*) - n_0 n_2 (\mathbf{n}_0 \mathbf{e}_2^*) (\mathbf{n}_2 \mathbf{e}_0) \} + \\ &\quad n_2 (\mathbf{n}_2 \times \mathbf{e}_2^*)_z \{ [n_0 n_1 (\mathbf{n}_0 \mathbf{n}_1) - 1] (\mathbf{e}_0 \mathbf{e}_1^*) - n_0 n_1 (\mathbf{n}_0 \mathbf{e}_1^*) (\mathbf{n}_1 \mathbf{e}_0) \} \end{aligned}$$

and

$$\mathcal{D} = e_{0z} (n_1 \mathbf{n}_1 - n_2 \mathbf{n}_2) (\mathbf{e}_1^* \times \mathbf{e}_2^*) + e_{1z}^* (n_0 \mathbf{n}_0 - n_2 \mathbf{n}_2) (\mathbf{e}_0 \times \mathbf{e}_2^*) + e_{2z}^* (n_0 \mathbf{n}_0 - n_1 \mathbf{n}_1) (\mathbf{e}_0 \times \mathbf{e}_1^*)$$

The matrix element can be expressed as

$$S = -i \frac{2\alpha^3}{(2\pi)^2} (4\pi)^{3/2} \omega \omega_1 \omega_2 \mathcal{M} (2\pi)^4 \delta(\sum \omega_i) \delta(\sum \mathbf{k}_i) \quad (25)$$

where

$$\mathcal{M} = \frac{B^3}{315} M_6 + \frac{B}{45\alpha^2} M_4. \quad (26)$$

3.2. Polarization selection rules

In the vacuum, polarization of the normal modes is linear, i.e.:

$$\begin{aligned} \mathbf{n} &= (\cos \theta, 0, \sin \theta) \\ \mathbf{e}_{\parallel} &= (\sin \theta, 0, -\cos \theta) \\ \mathbf{e}_{\perp} &= (0, 1, 0). \end{aligned} \quad (27)$$

Functions $\mathcal{C} = 0$ and \mathcal{D} vanish when we neglect refraction, while otherwise they are of the order of $n - 1$. Using equations (27) and neglecting refraction we find that M_4 vanishes while

$$\begin{aligned} M_6(\perp \rightarrow \perp + \perp) &= 48 \sin^3 \theta \\ M_6(\perp \rightarrow \parallel + \parallel) &= 26 \sin^3 \theta \\ M_6(\parallel \rightarrow \perp + \parallel) &= 26 \sin^3 \theta, \end{aligned}$$

and $M_6 = 0$ for all other transitions.

In the presence of matter the functions \mathcal{C} and \mathcal{D} no longer vanish. This is due to the fact that, in general, the refraction coefficients differ from unity, polarization vectors are elliptical rather than linear, photons in the process are not exactly collinear, and there exists a small degree of longitudinal polarization. The polarization related effects are the strongest for high matter density and propagation direction along the field.

3.3. Kinematic selection rules

The kinematic selection rules arise from the fact that for some transitions the the energy conservation cannot be satisfied. The kinematic selection rules can be discussed analytically using the dispersion relation $k = n(\omega, \mu)\omega \equiv (1 + \xi(\omega, \mu))\omega$. We note that the refraction coefficient is very close to unity, see Figures 1 and 2, and therefore for a given μ and one can invert the dispersion relation to obtain

$$\omega = (1 - \xi(k, \mu) + 0(\xi^2))k \quad (28)$$

We note that for the fixed initial photon the function $f \equiv \omega_0 - \omega_1 - \omega_2$ is monotonically decreasing with μ' - the cosine of the angle between the initial and one of the final photons. Thus, it suffices to verify that equation $f = 0$ has no solution for the collinear photons, to be sure that there are no solutions for non-collinear photons. Using momentum conservation and equation (28), one obtains for the collinear photons:

$$f_{\text{collinear}} = -\xi(\mathbf{k}_0, \mu_0)k_0 + \xi(k_1, \mu_0)k_1 + \xi(k_2, \mu_0)k_2 \quad (29)$$

The condition for the kinematic selection rules to be satisfied is $f_{\text{collinear}} > 0$.

In vacuum in the limit $\frac{\omega}{m} \ll 1$ the refraction coefficients are functions of the magnetic field and the dependence on photon energy ω is weak, see Figure 2. In this case condition (29) can be rewritten as $-\xi_0 + x\xi_1 + (1 - x)\xi_2 > 0$, where x is a number between 0 and 1. It is clear, that transitions $\parallel \rightarrow \parallel + \perp$ and $\parallel \rightarrow \perp + \perp$ are not allowed. Since in the first order in $\frac{\omega}{m}$ the functions ξ increase as a function of ω transitions $\parallel \rightarrow \parallel + \parallel$ and $\perp \rightarrow \perp + \perp$ are also forbidden. Thus in vacuum only two transitions are kinematically allowed: $\perp \rightarrow \perp + \parallel$ and $\perp \rightarrow \parallel + \parallel$.

Combining the polarization selection rules and the kinematic selection rules we conclude, in agreement with Adler, that only the transition $\perp \rightarrow \parallel + \parallel$ is allowed vacuum.

In the presence of matter the discussion of kinematic selection rules becomes more complicated since the refraction indices as a function of energy are rather complicated functions. The kinematic selection rules become complicated when the field is strong enough so that the electron cyclotron resonance influences refraction significantly. Around the resonance refraction coefficients are non monotonic functions of energy. In this case there may be a fraction of final state space that becomes kinematically allowed because of the influence of plasma on refraction coefficients.

3.4. Absorption coefficient

In the case of propagation in vacuum we ignore dispersion and calculate the integral of equation (21)

$$\int dr = \frac{2\alpha^6}{(2\pi)^3} |\mathcal{M}|^2 \times \int kk_1(k - k_1) k_1^2 dk_1 d\cos\theta d\phi \delta(k - k_1 - |\vec{k} - \vec{k}_1|) = \frac{\alpha^6}{2\pi^2} |\mathcal{M}|^2 \frac{\omega^5}{30}.$$

Due to the selection rules discussed above the only non-vanishing photon splitting absorption coefficients is

$$r(\perp \rightarrow \parallel + \parallel) = \frac{\alpha^6}{2\pi^2} B^6 \sin^6 \theta \frac{\omega^5}{30} \left(\frac{26}{315} \right)^2,$$

in full agreement with the result obtained by Adler (1971).

In general, when the polarization modes are not linear and we take into account the dispersion relation equation (21) can be written as

$$r = \frac{2\alpha^6}{(2\pi)^3} \int |\mathcal{M}|^2 \omega \omega_1 \omega_2 k_1^2 dk_1 d\cos\theta' d\phi' \delta(\omega - \omega_1 - \omega_2) \quad (30)$$

where we wrote explicitly the variables in the system U' and ω -s are function of k and μ . Defining $f \equiv \omega_0 - \omega_1 - \omega_2$, we can integrate over $\cos\theta'$ and obtain

$$r = \frac{2\alpha^6}{(2\pi)^3} \int_0^k dk_1 k_1^2 \int_0^{2\pi} d\phi' \omega \omega_1 \omega_2 |\mathcal{M}|^2 \left| \frac{df}{d\mu} \right|_{f=0}^{-1}, \quad (31)$$

which can be evaluated numerically. The integrand in equation (31) is understood to vanish whenever there is no solution of equation $f = 0$.

4. Results

We evaluate equation (31) numerically to obtain the photon splitting absorption coefficient for different polarization channels, and various photon energies, magnetic fields and plasma densities. In the calculation we use the refraction indices of equation (3), the polarization vectors given by equation (8), and calculate the matrix element using equation (26). At each integration point we evaluate the function f and find whether the energy conservation is satisfied.

We present the results in Figures 3, 4, 5, and 6. Each figure consists of four panels which show the splitting rates for four angles of propagation with respect to the magnetic field: 10° , 20° , 30° , and 70° . Figures 3, 4 show the splitting absorption coefficient as a function of matter density of a photon with the energy $\hbar\omega = 1.5m_ec^2$; Figure 3 for the case $B = B_c$ and Figure 4 for the case $B = 2B_c$. We present photon splitting absorption coefficients as functions of energy when the plasma density is 100g cm^{-3} in for $B = B_c$ in Figure 5, and for $B = B_c$ in Figure 6. We show the photon splitting absorption coefficients for the energies below $2m_ec^2$ since above this energy the opacity is dominated by the single photon pair production.

We first consider the effects of matter density on the photon splitting rates. At low densities the influence of matter is negligible, and we recover the vacuum case when all the polarization vectors are linear, and the kinematic selection rules are determined by the magnetic vacuum refraction. With the increase of density polarization of the normal modes becomes elliptical starting at the photons propagating near to the direction of the field. At small angles this effects are pronounced already at the density of 0.1g cm^{-3} . However comparing Figures 4 and 5 we see that the dominant effect is due to the kinematic selection rules and the influence of the electron cyclotron resonance is crucial. This is also clearly seen in Figure 6, where a number of splitting channels that are forbidden in vacuum suddenly turns on for energies above the cyclotron resonance.

At a low value of the magnetic field the process rapidly becomes unimportant, since the rate scales B^6 . With the increasing value of the magnetic field the plasma effects start to be important when the electron cyclotron resonance falls right around the electron mass, i.e. the field has a value close to the critical field. In these case when the matter is sufficiently dense the effects of the electron cyclotron resonance influence the kinematic selection rules significantly thus allowing more photon splitting polarization channels. When the value of the magnetic field is higher than $2B_c$ the electron cyclotron resonance falls above region of integration over the final states and the does not influence the splitting rate. Moreover with the increasing magnetic field refraction becomes dominated by the vacuum terms, and the effects of plasma become less and less important.

Figures 5 and 6 show the effects of photon energy on the splitting absorption coefficient. When the electron cyclotron resonance effects are ignored only small frequencies and small angles of propagation are influenced, since it is there where the refraction coefficients and the polarization of the normal modes are the most influenced by plasma. However this is also the region where the photon splitting coefficient is the smallest, see equation (1).

5. Discussion

In this work we extend the results of Adler (1971) to the case of propagation in the magnetized plasma and concentrate on the case of the density typical for a neutron star atmosphere. Our approach is accurate for the magnetic fields up to approximately the critical field since we use

a low field approximation in the calculation of the matrix element. We calculate the refraction coefficients accurately and thus the kinematic selection rules do not suffer from this limitation.

We have calculated the photon splitting absorption coefficient as a function of magnetic field, plasma density, and the photon energy and direction. We have found a region of the parameter space (density $\rho > 1 \text{ g cm}^{-3}$, the magnetic field $0.1B_c < B < 2B_c$, propagation angles $\theta < 30^\circ$) where the effects of plasma are the most pronounced. A part of these region is where the photon splitting absorption is small, so the region of importance is limited to photon energies above $m_e c^2$. We find that the the photon splitting rate is well described by the vacuum approximation in the remaining part of the parameter space.

Photon splitting absorption coefficient is small when compared to other processes that may play a role in plasma, for example the electron scattering opacity is $k_{scat} = 0.4(\hbar\omega/m_e c^2)^2(B_c/B)^2(\rho/\text{g cm}^{-3})\text{cm}^{-1}$ for the extraordinary mode, a value a few orders of magnitude higher than that for photon splitting. Thus photon splitting can play a significant role only in very special astrophysical cases. An example of such environment could be in deep layers of a neutron star atmosphere. Therefore the results presented here may apply to soft gamma-ray repeaters, where a large amount of energy is deposited in the crust of a neutron star. Photon splitting in a high density plasma may be a way of producing a large number of soft X-ray photons which later on escape. Our results can also be applied to the high energy radiation from isolated neutron stars provided that we see radiation from the surface and not the magnetosphere. However, the main conclusion is that surprisingly the effects due to the presence of plasma are important in a rather small fraction of the parameter space and the vacuum approximation can be used in most calculations.

Acknowledgements. This work was supported by the following grants KBN-2P03D00911, NASA NAG 5-4509 and NASA NAG 5-2868. The author thanks Victor Bezchastnov for assistance in calculating the matrix elements, and George Pavlov, Don Lamb and Cole Miller for many helpful discussions during this work.

REFERENCES

Adler S. L. 1971, Ann. Phys. 67, 599.

Baier, V. N., Milshtein, A. I. Shaisultanov, R. Zh., 1996, Phys. Lett. 77, 1695.

Berestetskii, V. B., Lifshits, E. M., and Pitaevskii, L. P., 1982 Quantum Electrodynamics, Oxford, Pergamon Press

Baring, M. G., 1995, ApJ, 440, L69.

Baring, M. G., Harding, A. K., 1997, ApJ, 482, 372.

Białynicka-Birula Z., Białynicki-Birula I., 1970, Phys. Rev. D. 2, 2341

Bulik, T. Miller, M.C. 1997, MNRAS, 288, 596.

Ginzburg V.L., Ruchadze A.A., 1975, 'Volny v magnitoaktivnoj plazmie, Nauka: Moscow

Gnedin Yu. N., Pavlov, G. G. 1974, Soviet Phys. JETP, 38, 903.

Harding, A. K., Baring M. G., Gonthier, P. L., 1997, ApJ, 476, 246.

Kouveliotou, C., etal. IAU Circ. 6944

Mentzel, M., Berg, D., Wunner, G., 1994, Phys Rev D, 50 1125.

Mészáros, P., 1992 High-Energy radiation from magnetized Neutron Stars, Univ. Chicago Press, Chicago.

Papanyan, V. O., Ritus, V.I., 1072, Soviet Phys. - JETP Lett., 34 1195.

Pavlov, G. G., Shibanov, Yu, A., Yakovlev, D., 1980, Ap&SS, 73, 33

Stoneham, R. J., 1979, J.Phys. A, 12 2187.

Thompson, C., Duncan, R., 1995, MNRAS, 275, 255.

Tsai, W., Erber, T., 1974, Phys. Rev. D, 10, 492.

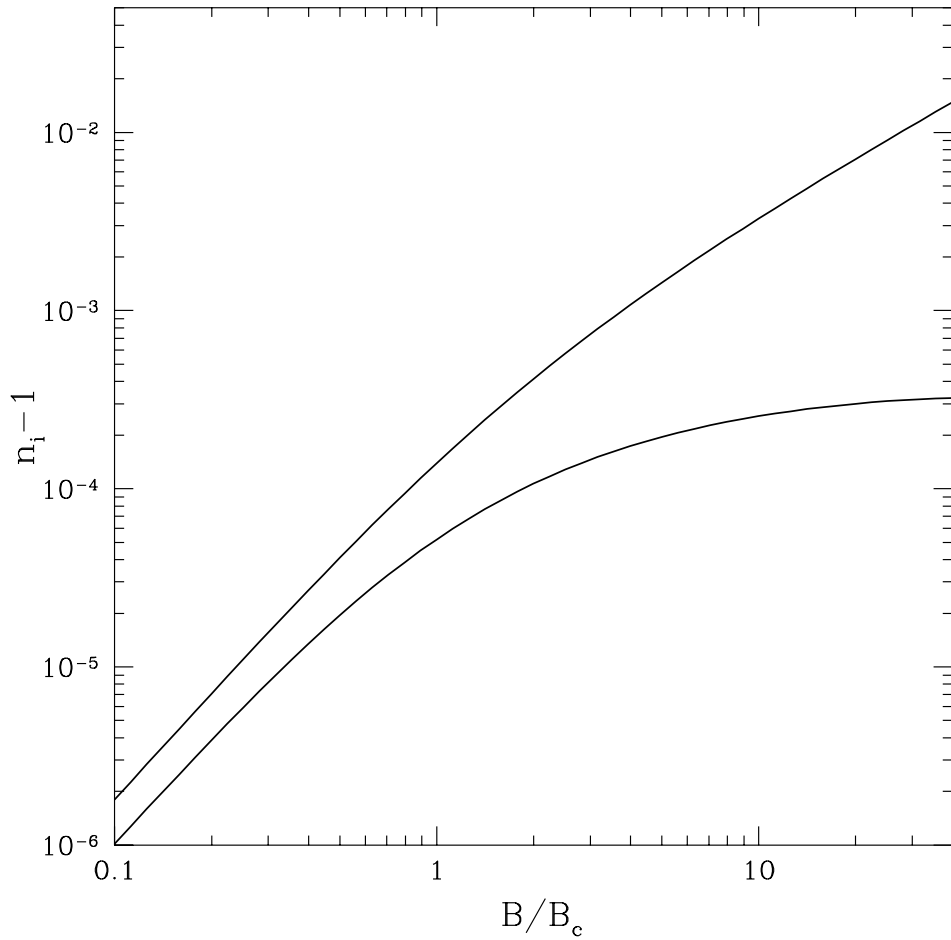


Fig. 1.— Refraction coefficients in magnetized vacuum as a function of the magnetic field, for propagation angle of 90° . The upper line corresponds to the \perp mode and the lower curve to the \parallel mode.

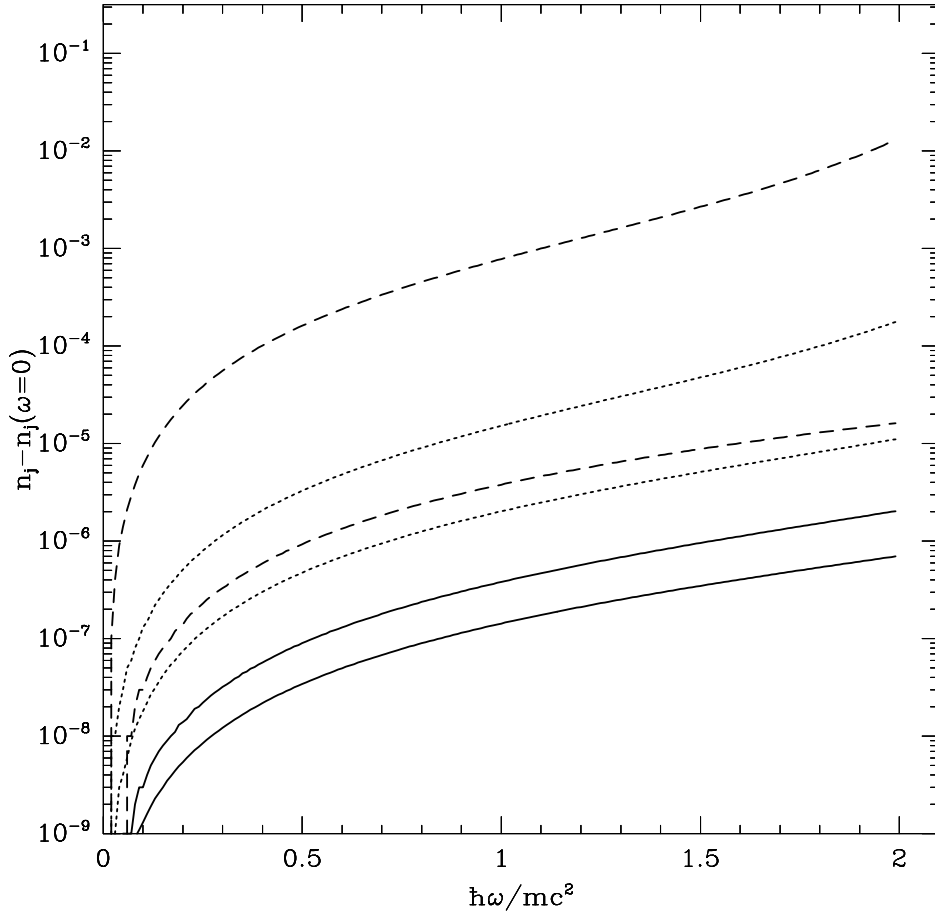


Fig. 2.— Refraction coefficients in magnetized vacuum as a function of photon energy for three values of the magnetic field: $B = 0.3 \times B_c$ (solid lines), $B = B_c$ (dotted lines), and for $B = 10 \times B_c$ (dashed lines). For each magnetic field the upper line corresponds to the \perp mode and the lower curve to the \parallel mode. The direction of propagation is perpendicular to the magnetic field. Note that at photon energies above $m_e C^2$ the low energy approximation $n - n(\omega = 0) \propto \omega^2$ no longer holds, especially for the very strong field case.

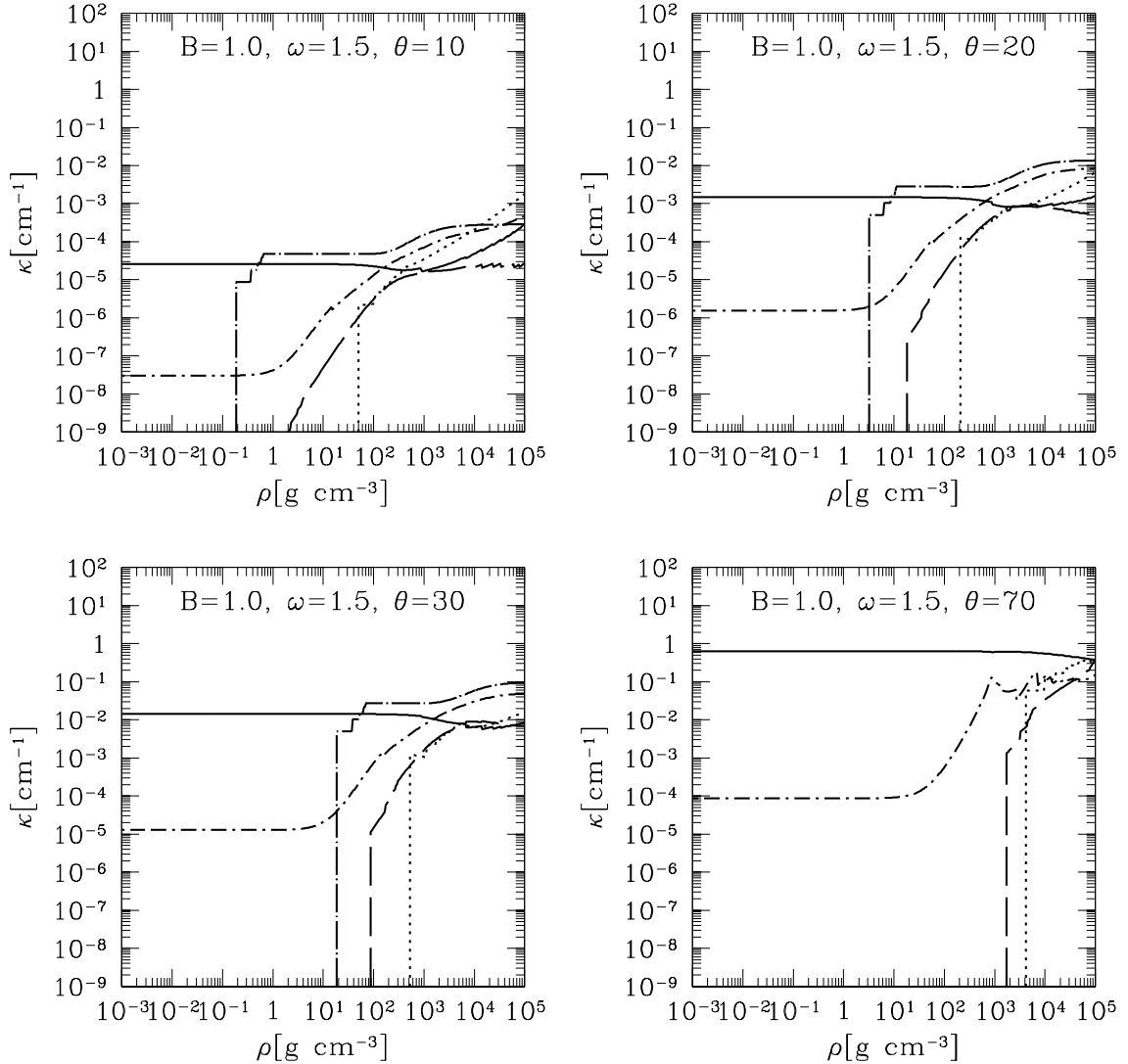


Fig. 3.— Photon splitting absorption coefficient as a function of density in plasma for $B = B_c$. The solid line corresponds to the case $1 \rightarrow 2 + 2$, i.e. the transition allowed in vacuum, the dotted line represents the transition $2 \rightarrow 1 + 2$, the long dashed $2 \rightarrow 2 + 2$, the short dashed dotted $1 \rightarrow 2 + 1$, and the long dashed dotted $1 \rightarrow 1 + 1$

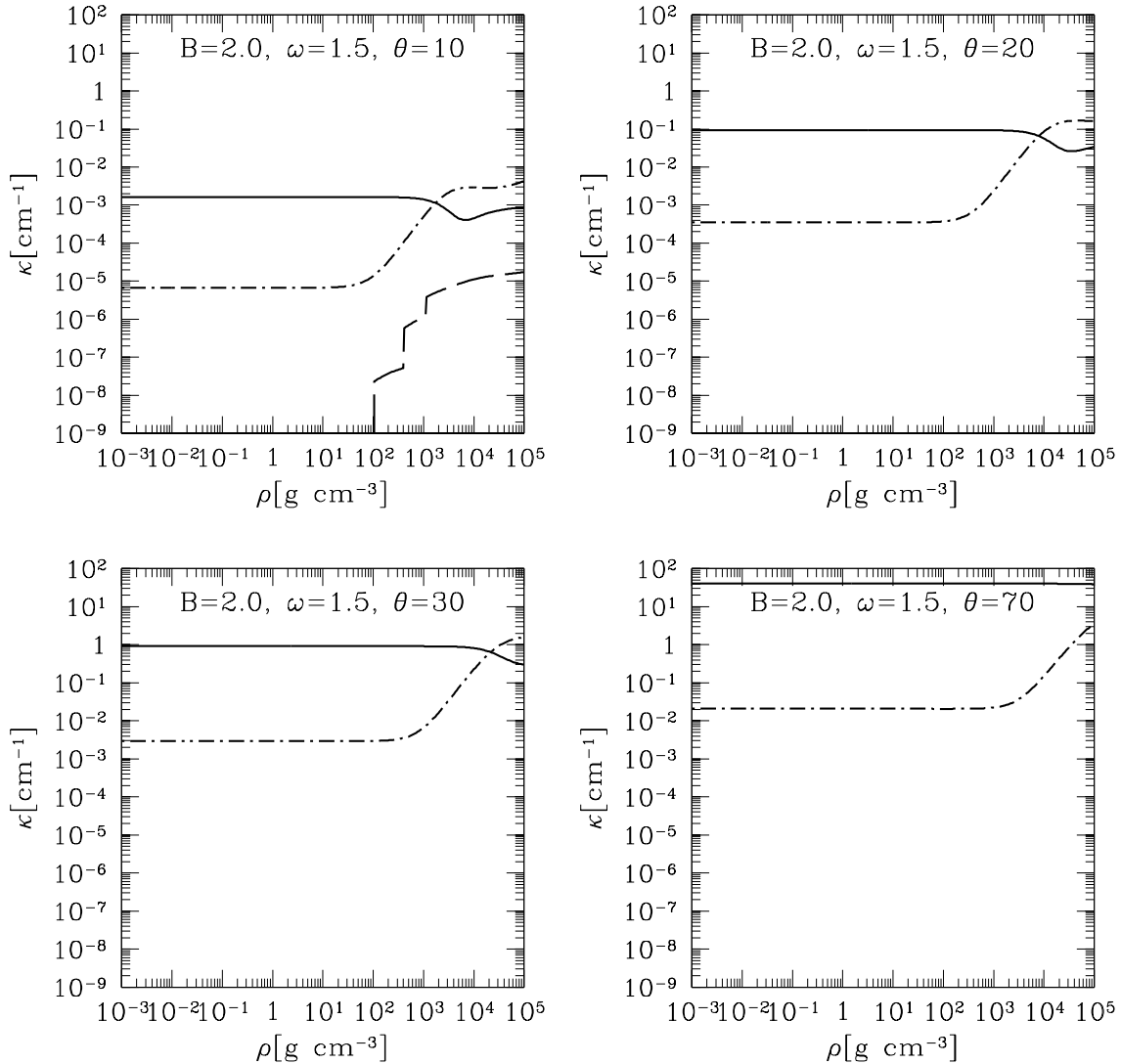


Fig. 4.— Photon splitting absorption coefficient as a function of density in plasma for $B = 2 B_c$. For explanation see Figure 3.

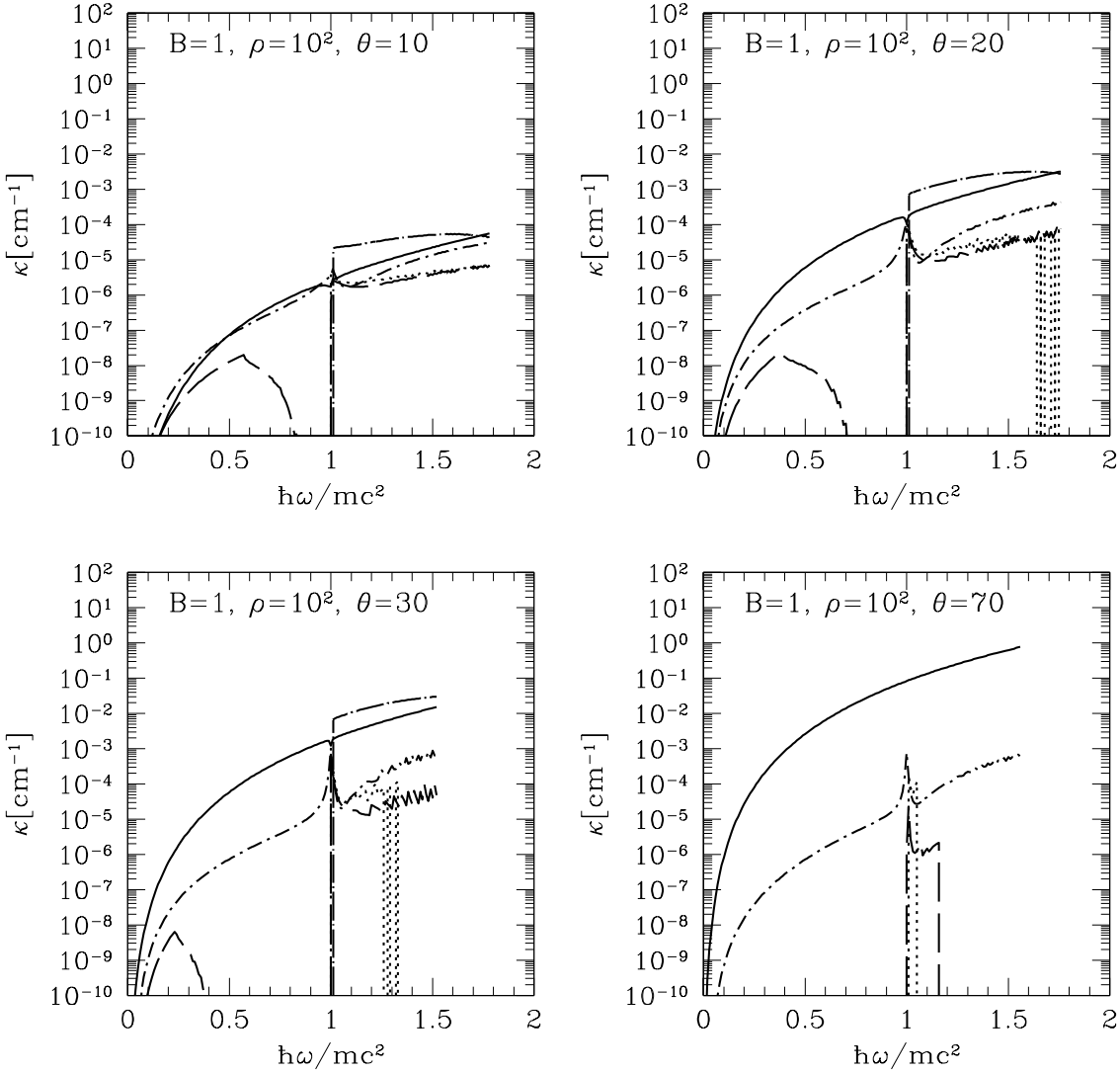


Fig. 5.— Photon splitting absorption coefficient as a function of energy in plasma with density 100 g cm^{-3} for $B = B_c$. For explanation see Figure 3.

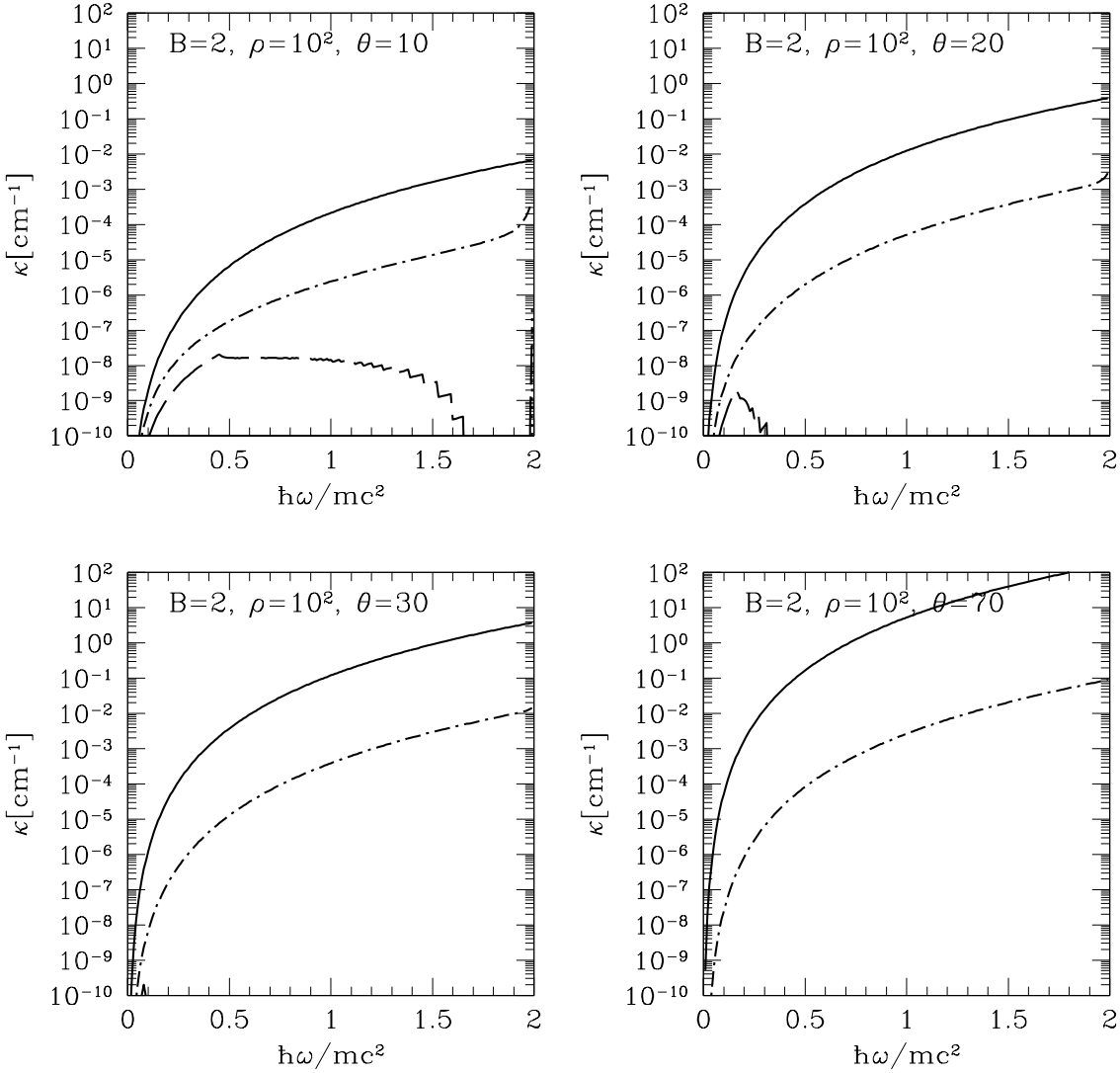


Fig. 6.— Photon splitting absorption coefficient as a function of energy in plasma with density 100 g cm^{-3} for $B = 2 B_c$. For explanation see Figure 3.